Molecular Diversity
https://doi.org/10.1007/s11030-019-09974-z

ORIGINAL ARTICLE

Synthesis, molecular docking and evaluation of novel sulfonyl hydrazones as anticancer agents and COX-2 inhibitors

Sevil Şenkardeş[1] · M. İhsan Han[2] · Necla Kulabaş[1] · Mürüvvet Abbak[3] · Özge Çevik[4] · İlkay Küçükgüzel[1] · Ş. Güniz Küçükgüzel[1]

Received: 20 March 2019 / Accepted: 4 July 2019

Abstract

In trying to develop new anticancer agents, a series of sulfonylhydrazones were synthesized. All synthesized compounds were checked for identity and purity using elemental analysis, TLC and HPLC and were characterized by their melting points, FT-IR and NMR spectral data. All synthesized compounds were evaluated for their cytotoxic activity against prostate cancer (PC3), breast cancer (MCF-7) and L929 mouse fibroblast cell lines. Among them, *N*′-[(2-chloro-3-methoxyphenyl) methylidene]-4-methylbenzenesulfonohydrazide **(3k)** showed the most potent anticancer activity against both cancer cells with good selectivity ($IC_{50} = 1.38$ µM on PC3 with SI = 432.30 and $IC_{50} = 46.09$ µM on MCF-7 with SI = 12.94). Further investigation confirmed that **3k** displayed morphological alterations in PC3 and MCF-7 cells and promoted apoptosis through down-regulation of the Bcl-2 and upregulation of Bax expression. Additionally, compound **3k** was identified as the most potent COX-2 inhibitor (91% inhibition) beside lower COX-1 inhibition. Molecular docking of the tested compounds represented important binding modes which may be responsible for their anticancer activity via inhibition of the COX-2 enzyme. Overall, the lead compound **3k** deserves further development as a potential anticancer agent.

The research was partly presented at the 6th International Bahçeşehir University (BAU) Drug Design Congress on 13–15 December 2018, İstanbul, Turkey.

Electronic supplementary material The online version of this article (https://doi.org/10.1007/s11030-019-09974-z) contains supplementary material, which is available to authorized users.

✉ Sevil Şenkardeş
sevil.aydin@marmara.edu.tr

[1] Department of Pharmaceutical Chemistry, Faculty of Pharmacy, Marmara University, Haydarpaşa, 34668 İstanbul, Turkey

[2] Department of Pharmaceutical Chemistry, Faculty of Pharmacy, Erciyes University, Kayseri, Turkey

[3] Scientific Technology Research and Application Centre, Adnan Menderes University, Aydın, Turkey

[4] Department of Biochemistry, School of Medicine, Adnan Menderes University, Aydın, Turkey

Published online: 13 July 2019

Graphic abstract

Sulfonylhydrazones was synthesized and *N*′-[(2-chloro-3-methoxyphenyl)methylidene]-4-methylbenzenesulfonohydrazide (**3k**) was identified as the most potent anticancer agent and COX-2inhibitor. In addition, this compound docked inside the active site of COX-2 succesfully.

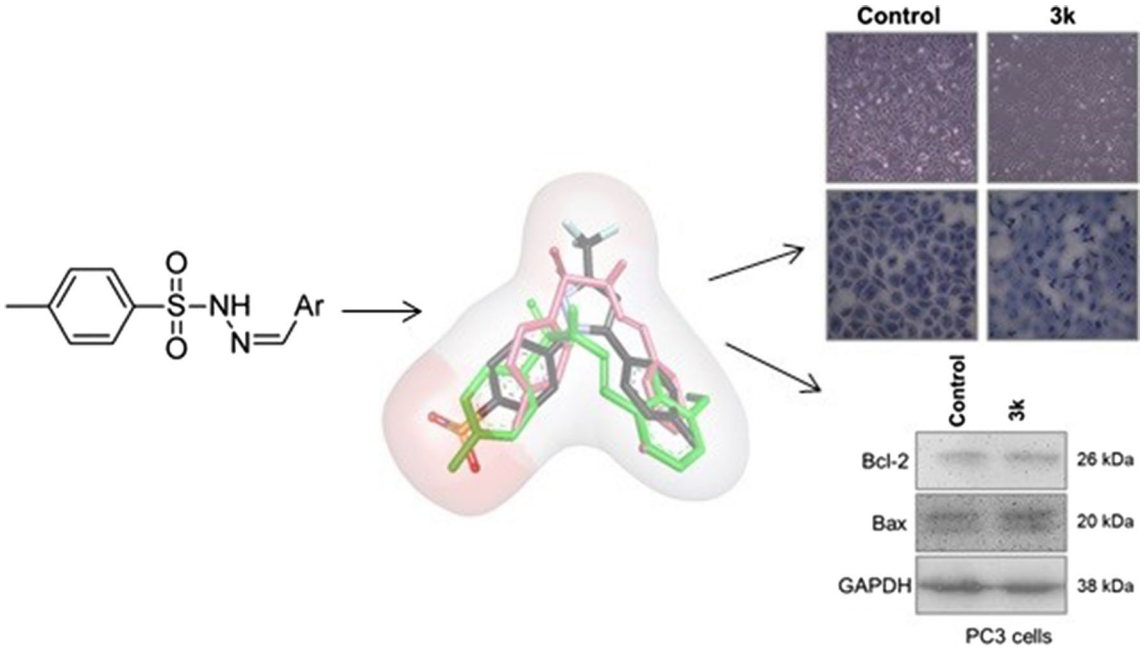

Keywords Anticancer activity · Apoptosis · Cyclooxygenase · Molecular docking · Sulfonylhydrazones

Introduction

Cancer is a major leading cause of death all over the world since the beginning of the twenty-first century, and the economic effect of this disease is important and increasing. Disease can develop various organs and systems of body at any age with no certain etiopathology. Among the anticancer therapies, chemotherapy receives much attention due to its effects on tumor cells. However, many anticancer drugs display serious adverse effects and toxicity; there is an urgent need to identify new compounds to fight against the fatal disease [1].

Apoptosis, or programmed cell death, is an important process crucial for elimination of unnecessary or unwanted cells. The feature of cancer is the ability of malignant cells to escape from apoptosis [2]. Many compounds that have been found to be a potential source of novel anticancer drugs show their antitumor activity by inducing apoptosis. Apoptosis induction occurs via extrinsic and intrinsic pathways [3]. The extrinsic pathway contains the binding of ligands to cell surface "death receptors" [4]. In the intrinsic pathway, anti-apoptotic Bcl-2 and proapoptotic Bax genes expression are key regulators at the mitochondria. As long as a drug alters the expression of apoptotic proteins, it might induce the apoptosis in cancer cells [5].

Carcinogenesis mostly breaks through multistep processes containing various somatic gene alterations. In particular, prostate and breast cancers have been characterized by alterations of genes and proteins involved in proinflammatory pathways [6, 7]. Cyclooxygenase is a key enzyme in prostanoid biosynthesis including prostaglandins that are also involved in inflammation. Cyclooxygenase-2 isoform (COX-2), which is an important enzyme in prostaglandin synthesis, is induced in many cells by inflammatory mediators and plays important roles in the "inflammogenesis of cancer" [8]. Several studies have shown that COX-2 is overexpressed in solid malignancies including breast [9], prostate [10] and colon [11] cancers. Recently, studies have shown a notable correlation between the expression of COX-2 and inhibition of apoptosis, so COX-2 is an emerging drug target for cancer treatment [12].

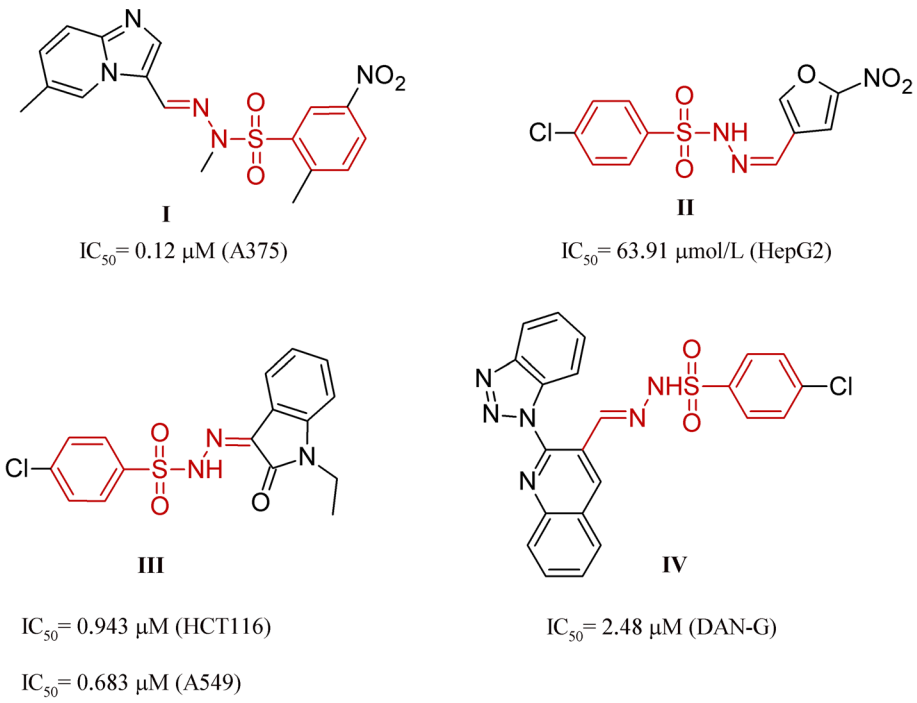

Fig. 1 Some reported anticancer agents bearing sulfonylhydrazone

In drug design strategy, small organic molecules play a critical role and act as extremely bioactive scaffolds. Hydrazone group, a prominent moiety present richly in medicinal molecules, has played a significant role in the development of different therapeutic agents. On the other hand, various biological [13] and chemotherapeutic activities of hydrazones [14–18] suggest them as an important pharmacophoric character. In particular, sulfonylhydrazones have been recognized as potential antimicrobial [19], antifungal [20], antiurease [21] and MAO inhibitory [22] activities, and as illustrated in Fig. 1, numerous sulfonylhydrazones have been recognized as potential anticancer agents such as compounds I and II which showed a significant anticancer activity against melanoma and liver cancer cell lines [23, 24], compounds III exhibited displayed high anticancer activities against HCT116 colon cancer and A549 lung cancer cell lines [25], and compound IV bearing benzotriazole ring was powerfully effective against DAN-G pancreas cancer cell line [26] (Fig. 1).

On the basis of aforementioned findings, herein some new sulfonylhydrazones have been synthesized and evaluated for their potential anticancer, apoptosis-inducing and COX enzyme activities. Also, the designed compounds were docked into COX-1 and COX-2 enzymes in order to examine the COX-1/2 selectivity and probable binding modes of derivatives inside the active site.

Results and discussion

Chemistry

The synthesis of sulfonylhydrazones **(3a–o)** followed the general pathway outlined in Scheme 1. In the initial step, p-toluenesulfonyl hydrazide **(2)** was synthesized via the reaction of tosyl chloride **(1)** and hydrazine hydrate in THF. The reaction of p-toluenesulfonyl hydrazide **(2)** with substituted aldehydes afforded 4-methyl-*N*′-(arylmethylidene)benzenesulfonyl hydrazides **(3a–o)**. The IR, ^{1}H-NMR and ^{13}C-NMR data were in agreement with the proposed structures of compounds. Among the newly synthesized compounds, compounds **3i** and **3n** have been reported previously [27, 28] and compound **3g** has got only a CAS number (CAS No: 461716-16-5) with no spectroscopic data. So, we presented full structural characterization not reported in the above-mentioned literature, including melting point, NMR data and elemental analysis.

The HMBC spectra of **3g** chosen as a prototype were very useful for locating the tertiary and quaternary carbons by identifying the various protons interacting with them through two-bond, three-bond and occasionally four-bond couplings as displayed in Fig. 2. Based on the HMBC spectrum, the correlations between H-1 (δH = 2.36) and C-2 (δC = 144.03), the correlations between H-3 (δH = 7.41) and C-1, C-2, [δC = 21.43 (C-1), 144.03 (C-2), the correlations between H-4 (δH = 7.76) and C-2 (δC = 144.03), the correlations between H-6 (δH = 7.92) and C-7, C-8, C-12 [δC = 126.78 (C-7), 123.56 (C-8), 132.61 (C-12)], the

Scheme 1 The synthetic route for compounds **3a–o**

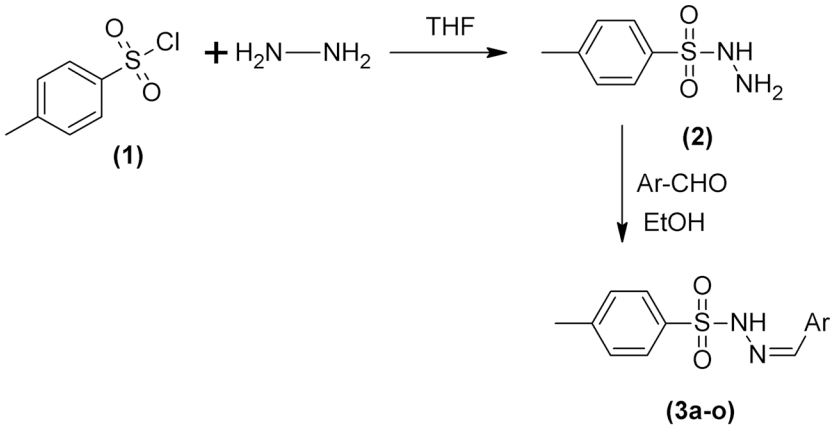

Comp.	R	Comp.	R
3a	2,2-difluoro-1,3-benzodioxol-5-yl	**3i**	5-bromo-2-methoxyphenyl
3b	4-bromothiophen-2-yl	**3j**	4-fluoro-2-(trifluoromethyl)phenyl
3c	4-phenylthiophen-2-yl	**3k**	2-chloro-3-methoxyphenyl
3d	4-fluoro-3-phenoxyphenyl	**3l**	2-chloro-6-methylphenyl
3e	2-chloro-3-(trifluoromethyl)phenyl	**3m**	6-bromopyridin-2-yl
3f	4-fluoro-3-methoxyphenyl	**3n**	1-methyl-1*H*-pyrrol-2-yl
3g	4-methoxy-3-nitrophenyl	**3o**	2-(trifluoromethoxy)phenyl
3h	3-phenyl-1*H*-pyrazol-4-yl		

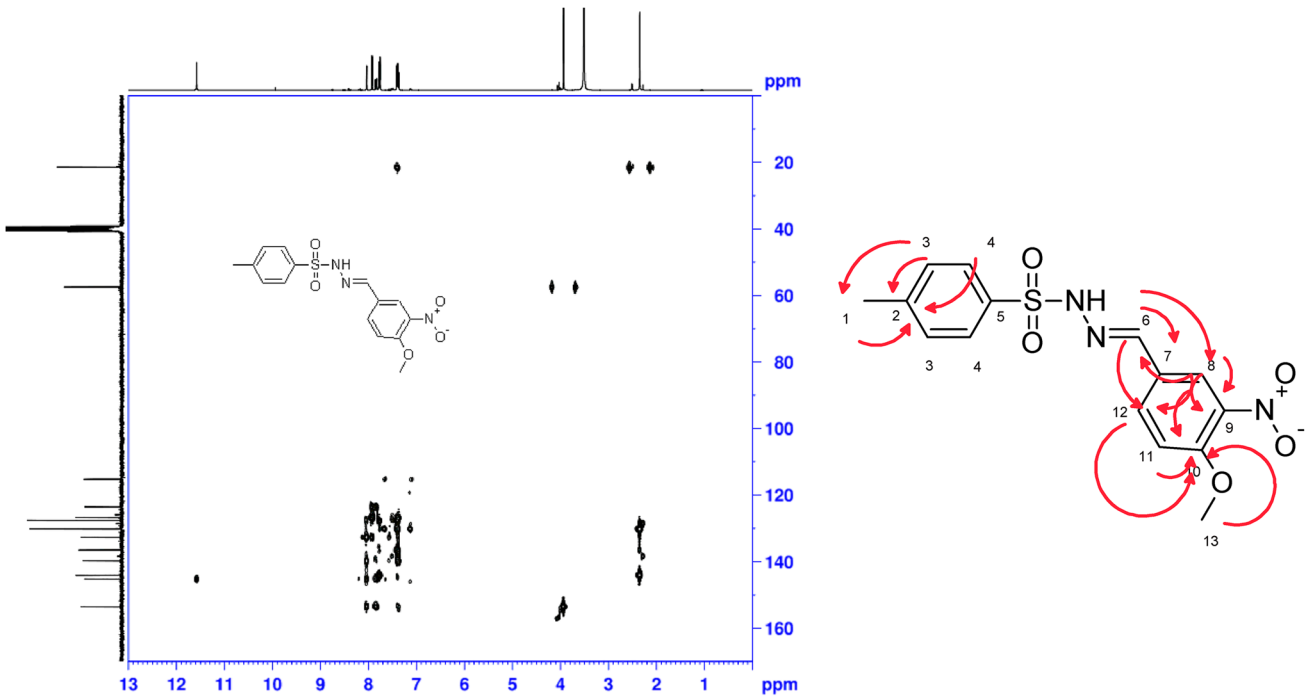

Fig. 2 HMBC spectrum and (H to C) interactions in compound **3g**

correlations between H-8 (δH = 8.04) and C-6, C-9, C-10, C-12 [δC = 145.19 (C-6), 139.72 (C-9), 153.45 (C-10), 132.61 (C-12)], the correlations between H-11 (δH = 7.39) and C-10 (δC = 153.45), the correlations between H-12 (δH = 7.85) and C-8, C-10 [δC = 123.56 (C-8), 153.45 (C-10)] and the correlations between H-13 (δH = 3.94) and C-10 (δC = 153.45) indicated the structure of **3g** should be as shown in Fig. 2.

Table 1 *In vitro* cytotoxic effect of compounds **3a–o** against human cancer cell lines and a normal cell line

Compound	IC_{50} (μM)				
	PC3	MCF-7	L929	SI* (PC3)	SI* (MCF-7)
2	99.20	176.18	154.57	1.55	0.87
3a	70.65	66.23	164.30	2.32	2.48
3b	66.20	140.29	240.68	3.63	1.71
3c	713.59	29.89	331.50	0.46	11.09
3d	173.63	529.80	ND	ND	ND
3e	43.77	287.77	7.49	0.17	0.02
3f	341.61	28.31	155.10	0.45	5.48
3g	188.05	360.43	ND	ND	ND
3h	138.09	405.18	10.20	0.07	0.025
3i	23.77	181.34	324.60	13.66	1.78
3j	28.33	283.25	314.90	11.12	1,11
3k	1.38	46.09	596.58	432.30	12.94
3l	143.17	167.95	920.03	6.42	5.47
3m	189.06	204.69	ND	ND	ND
3n	314.40	114.30	0.99	0.003	0.006
3o	35.39	104.09	ND	ND	ND
Celecoxib	150.00	128.01	523	3.4	4.08
Cisplatin	3.3*	22.2*			

ND not determined, *Lit: [31]

SI: IC_{50} for L929 cell line/IC_{50} for PC3 and MCF-7 cell line

Table 2 The in vitro COX inhibition percentages and docking results of the active compounds

Compound	COX-1		COX-2	
	Inhibition % (50 μM)	Binding affinity ΔG (kcal/mol)	Inhibition % (50 μM)	Binding affinity ΔG (kcal/mol)
2	26	n.t.	25	n.t.
3a	13	n.d.	41	−7.3
3b	29	−6.2	20	−6.7
3c	49	−8.1	75	−7.6
3d	76	−8.5	14	−6.9
3e	43	−7.1	11	−7.1
3f	56	−7.9	80	−8.0
3g	69	−8.5	19	−6.7
3h	82	−8.7	13	−7.2
3i	28	−6.8	82	−8.0
3j	64	−8.1	73	−7.8
3k	48	−7.7	91	−8.6
3l	63	−8.0	64	−7.0
3m	56	−7.5	88	−8.4
3n	16	n.d.	22	−7.2
3o	32	−7.4	64	−7.0
Celecoxib	92	−10.5	100	−12.0

n.d. not determined, *n.t.* not tested

Anticancer activity

The anticancer activity of the synthesized compounds was evaluated on two human cancer cell lines, namely human breast adenocarcinoma cell line (MCF-7), prostate cell line (PC-3) and mouse normal fibroblasts (L929) using MTT assay.

The four compounds **3i–k** and **3o** demonstrated potent antiproliferative activity against PC3 cell line, and compounds **3c**, **3f** and **3k** demonstrated potent antiproliferative activity against MCF-7 cell line. The starting compound **2** did not show promising anticancer activity against both cancer cells.

Moreover, compound **3k** showed the most promising effects for both tumor cell lines with lower IC_{50} values (IC_{50} = 1.38 μM against PC3 cell and IC_{50} = 46.09 μM against MCF-7 cell). The ideal anticancer drug candidate should be cytotoxic to cancer cells and be harmless for normal cells. The toxicity profiles of compounds were determined against L929 cells indicating a considerable safety profile. The IC_{50} and selectivity index (SI) results of the compounds are presented in Table 1. Strikingly, the results propose that active derivatives clearly are more cytotoxic to cancer cells than the tested normal cell L929 according to the selectivity index values. The most selective compound **3k** has SI yielding 432.30 for PC3, and 12.94 for MCF-7 cell line.

Celecoxib was used as a positive control because its selective COX-2 inhibition correlated with induction of apoptosis in several cancer models, anticancer properties [29, 30], and it is the bound ligand of COX-2 enzyme used in our molecular modeling studies. Cisplatin has been one of the most widely used chemotherapeutic drugs and has been used in clinics for the treatment of various cancers. Altaf et al. reported the cytotoxicity values of cisplatin against PC3 and MCF-7 cell lines with IC_{50} values of 3.3 and 22.2 μM, respectively [31]. Compared with data, the lead compound **3k** showed potent anticancer activity superior to those of celecoxib and cisplatin.

In vitro COX-1/2 inhibitory activities

It is well known that COX-2 plays a critical role in a number of solid tumors. Therefore, this enzyme is taken as a target for anticancer drug development. The results of the COX-1/2 inhibition studies of the compounds are listed in Table 2. Celecoxib, which was used as a positive control, provided 100% inhibition at 50 μM. In the present series, compounds **3c**, **3f**, **3i**, **3j**, **3k** and **3m** showed high COX-2 inhibition (73–91%) at a concentration of 50 μM

while the least active compounds like **3d** and **3h** with weak cyclooxygenase-2 inhibition potency. Conversely, **3d** and **3h** showed the highest COX-1 inhibitory activity (76% and 82%, respectively) with high selectivity and no anticancer effect. All synthesized compounds were less potent COX inhibitors than celecoxib.

Compound **3k** bearing 2-chloro-3-methoxyphenyl moiety is the most active derivative as COX-2 inhibitor by 91% inhibition (with a binding energy of -8.6 kcal/mol), while compound **3e** with 2-chloro-3-trifluoromethylphenyl moiety is the least active compound (11% inhibition with binding energy of -7.1 kcal/mol). These data indicated that the methoxy substituent at the meta-position of the phenyl rings is essential for their inhibitory activity. Moreover, compound **3d** bearing 4-fluoro-3-phenoxy showed 14% COX-2 enzyme inhibition while replacing the phenoxy group by methoxy on the phenyl ring increases the inhibition as seen in the compound **3f** displayed 80% inhibition.

According to the acquired data, there was a generally relationship between COX-2 enzyme inhibition and anticancer activity results. Compounds **3k** and **3i** that showed the highest COX-2 inhibition appeared as the most active anticancer agents, while the weak inhibitors **3h** and **3d** showed the lowest anticancer activity. Although celecoxib was the strongest COX-2 inhibitor in this study, it showed weak cytotoxicity against MCF-7 and PC-3 cell lines. This is because the inhibitory effect of celecoxib on the proliferation of breast and prostate cancer cells in vitro was observed in a dose- and time-dependent manner [30, 32]. For celecoxib, 4 days was required to achieve 37% cell growth inhibition against PC3 cell line at 5 µM [33]. The exact mechanisms for its anticancer activity are not clear yet, and Grosch et al. showed that celecoxib showed antiproliferative effect through COX-independent mechanisms [34].

While anticancer effect of COX-2 inhibitors depends on dose and time, this effect cannot be associated with COX-2 enzyme inhibition alone because COX-2 inhibitors show anticancer effects via COX-2-dependent and COX-2-independent pathways [35]. Among them, COX-2 inhibitors trigger apoptosis in cancer cell as a result of a decreased level of Bcl-2 protein. SC-58125, which is a derivative of celecoxib, induced apoptosis by down-regulation of Bcl-2 like lead compound **3k** [36], whereas celecoxib induced apoptosis independent of Bcl-2 down-regulation in various cancer cells [30]. The induction of apoptosis in cancer cells by COX-2 inhibitors is a unique process, and the increased COX-1/COX-2 selectivity may not display a correlated anticancer effect [30, 37]. As shown in Tables 1 and 2, compound **3m**, selective COX-2 inhibitor, did not show any significant anticancer activity in both cancer cell lines. Moreover, compound **3j**, which is less selective than **3m**, displayed notable cytotoxicity against PC3 cell line with an IC_{50} value of 28.33 µM.

Compound 3k inhibits cell proliferation and induced morphological changes

Herein, compound **3k** was chosen for further studies on the possible mechanism of its anticancer activity. MTT assay was performed to assess the effect of **3k** on PC3 and MCF-7 cell proliferation. When PC3 and MCF-7 cells were incubated with **3k** at IC_{50} values for 12, 24 and 48 h, the collected data suggested that compound **3k** decreased the viability of PC3 and MCF-7 cells in a time-dependent manner (Fig. 3). In addition, PC3 and MCF-7 cells treated with **3k** at IC_{50} value for 24 h were stained with crystal violet and cell growth inhibition and morphological changes were observed under inverted microscope. While both cell lines clearly exhibited an increase in cell number (Fig. 3, DMSO only control), treatment with compound **3k** gave rise to a marked decrease in cellular confluency such as reduction of cell population, reduction of cell volume, cell shrinkage and loss of cellular architecture.

Compound 3k induces apoptosis through mitochondrial pathway

To reveal the possible mechanisms responsible for the apoptotic effects of compound **3k**, we evaluated its effects on the expression level of a series of proteins related to mitochondrial apoptosis. Therefore, PC3 and MCF-7 cells were blotted for Bax and Bcl-2, following treatment with compound **3k** (Figs. 4a and 5a) and quantified (Figs. 4b–d and 5b–d). As expected, the proapoptotic Bax levels were increased in PC3 cells, and the level of increase in Bax expression was similar in response to MCF-7 cells. On the other hand, the decrease in Bcl-2 levels varied between the cells. While there was little to no change in Bcl-2 expression following compound **3k** treatment in cell lines, Bax/Bcl-2 ratio of cells treated with compound **3k**, expression levels were significantly increased in PC3 and MCF-7 cells.

In silico docking studies

Clinical studies have shown that COX-2 levels are increased in a number of human cancers and COX-2 isoenzyme released in cancer cells is an ideal drug target to inhibit carcinogenesis [38]. Computer-assisted molecular modeling techniques have been used to estimate the possible inhibitory activities and mechanism of binding to COX enzymes of the synthesized compounds. Trans-isomers of compounds **3a-o**

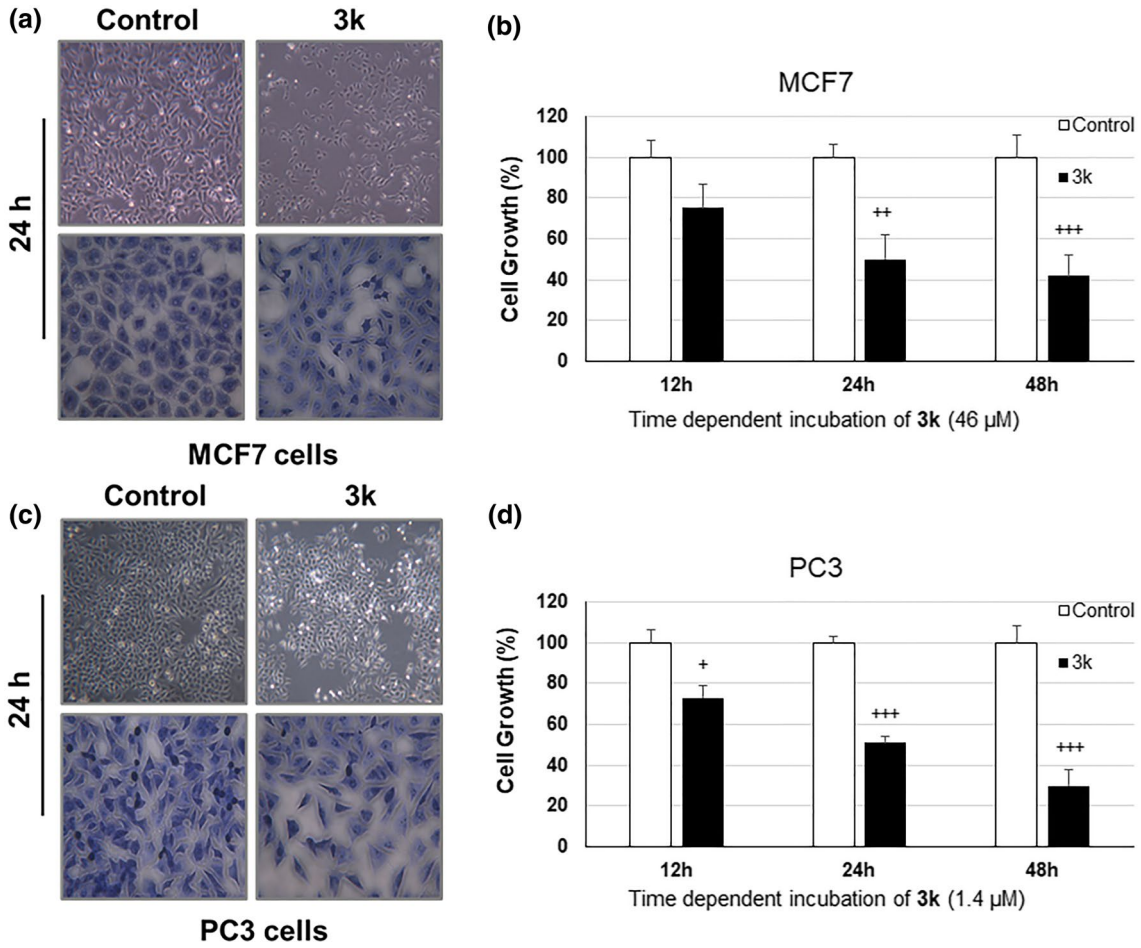

Fig. 3 Effect of compound **3k** on cell survival in human prostate cancer cells PC3 and human breast cancer cells MCF-7. **a** Effect of compound **3k** (46 µM) on cell growth of MCF-7 cells for 24 h. Morphological changes with bright light (up) and stained with crystal violet (down). **b** Percentage of cell growth in MCF-7 cells treated with **3k** (46 µM) for 12 h, 24 h, 48 h ($++p<0.01$, $+++p<0.001$ compared to control in MCF-7 cells). **c** Effect of compound **3k** (1.4 µM) on cell growth of PC3 cells for 24 h. Morphological changes with bright light (up) and stained with crystal violet (down). **d** Percentage of cell growth in PC3 cells treated with **3k** (1.4 µM) for 12 h, 24 h, 48 h ($++p<0.01$, $+++p<0.001$ compared to control in PC3 cells) ($+p<0.05$, $++p<0.01$, $+++p<0.001$ compared to control in PC3 cells)

were evaluated since they have more appropriate poses than cis-isomers in COX active site. Binding energy obtained from the docking studies of the compounds **3a**–**o** as well as celecoxib as reference ligand with COX-1 and COX-2 by using Autodock Vina is presented in Table 2.

The in silico studies were in agreement with the in vitro results where docking of hydrazone derivatives showed a relative selectivity of these derivatives to COX-II active site. Results of both in vitro enzyme inhibition assay and molecular modeling studies have shown that compounds **3k** and **3m** are the best COX-2 inhibitors among the synthesized compounds. When binding poses of both synthesized compounds and celecoxib were compared in active site, we detected highly similar orientations of compounds **3k**, **3m** and celecoxib (Fig. 6a). In addition, binding poses of compounds **3b** and **3g** with minimum binding affinity were compared with celecoxib in active site, and it was detected that these compounds have not appropriate orientation in binding pocket. The reason for the weak inhibition of these compounds was that they did not overlap with the ligand as shown in Fig. 6b.

When the interactions of compound **3k** with active site of COX-2 enzyme were examined, hydrogen bonds between sulfonyl group with side chains of both Tyr341 and Ser339 were detected. Moreover, we observed that while sulfonylhydrazone group formed backbone hydrogen bond with Val509, the methoxy group formed hydrogen bond with the side chain of Ser516, too. Also, contribution of pi-alkyl interaction of among methyl group and Val509 besides alkyl–alkyl weak interaction of between this group and Ala502 was observed. Finally, pi-alkyl hydrophobic interactions between phenyl ring which is substituted with

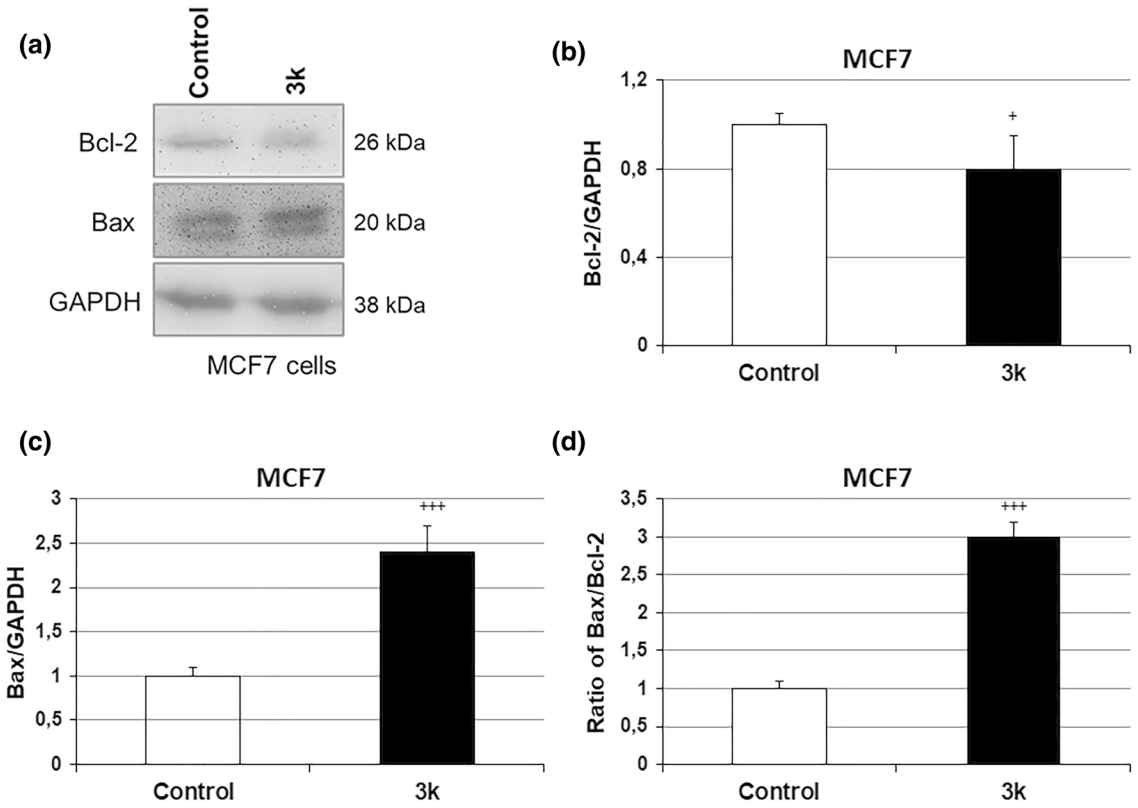

Fig. 4 Effects of **3k** on apoptotic proteins in breast cancer cells. **a** Effects of compound **3k** (46 µM) compound treatment at 24 h on the Bcl-2 and Bax proteins in MCF-7 cells, representatively. **b–d** Western blot densitometry analysis of expression levels of Bcl-2 and Bax proteins **c** Ratio of Bax/Bcl-2 expression in MCF-7 cells (++$p < 0.01$, +++$p < 0.001$ compared to control in MCF-7 cells). Each protein band was normalized to the intensity of GAPDH used

sulfonyl group and the side chains of Ser339 and Val509 are thought to contribute to the activity (Fig. 7).

As a result of these interactions, by holding constant the sulfonyl hydrazone core, substitution of electron-withdrawing groups on both phenyl rings may increase the H-bond interaction with Ser339, Leu338, Tyr341 and Ser516 as similar to celecoxib.

Molecular modeling studies have shown that compounds **3d** and **3h** are the best COX-1 inhibitors among the synthesized compounds as in the in vitro enzyme inhibition assay. Besides, no interaction could be detected between COX-1 active site and compounds showing below 20% inhibition during biological studies. Furthermore, for COX-2 selective compounds **3c**, **3f**, **3i**, **3k** and **3m**, in vitro enzyme inhibition assay and molecular modeling studies results were found to be correlated with each other.

In silico prediction of potential pharmacokinetic and toxicological properties

The in silico toxicity risks obtained by OSIRIS Data Warrior software (http://www.openmolecules.org/datawarrior/) and ADME properties calculated using SwissADME (http://www.swissadme.ch/) online tools are given in Table 3. Regarding in silico toxicity results for mutagenicity, tumorigenicity, irritant and reproductive effects, almost all synthesized compounds were predicted to be safe. The clogP is an important data indicating the lipophilicity and according to Lipinski's rule of five, the clogP value of ≤ 5 is necessity for a compound to be a drug candidate. Our results showed that cLogP values for the target compounds were well within the acceptable criteria. Polar surface area (PSA) values of the drug candidates have been shown to correlate very well with the human intestinal absorption, Caco-2 monolayer's permeability, and blood–brain barrier penetration and values of 140 or more are expected to exhibit poor intestinal absorption. The results show that all the compounds have optimal TPSA values. The aqueous solubility of a compound significantly affects its absorption and distribution characteristics. Typically, a low solubility means a bad absorption and suitable values for logS > 4 were observed for the hydrazones that were synthesized herein. The title compounds do not violate the Lipinski rule, and they fall well in the range (Table 3).

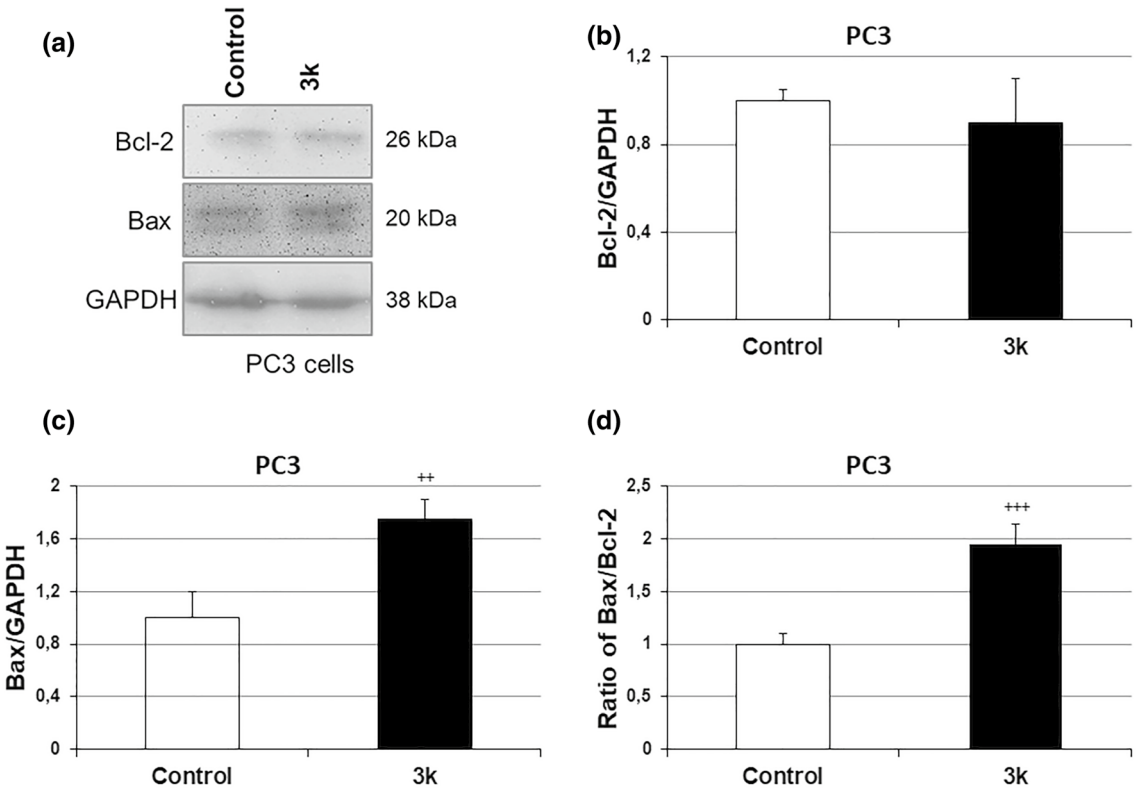

Fig. 5 Effects of **3k** on apoptotic proteins in prostate cancer cells. **a** Effects of compound **3k** (1.4 μM) treatment at 24 h on the Bcl-2 and Bax proteins in PC3 cells, representatively. **b-d** Western blot densitometry analysis of expression levels of Bcl-2 and Bax proteins. **c** Ratio of Bax/Bcl-2 expression in PC3 cells ($++p<0.01$, $+++p<0.001$ compared to control in PC3 cells). Each protein band was normalized to the intensity of GAPDH used

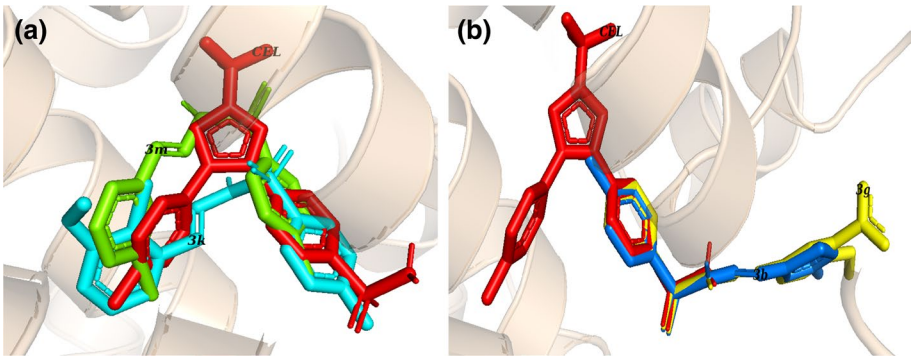

Fig. 6 The comparison of **a** orientations of most active compounds **3k** (cyan) and **3m** (green) **b** orientations of least active compounds **3b** (brown) and **3g** (black) with celecoxib (red) in COX-2 active site. (Color figure online)

Estimated intestinal absorption (%ABS) was calculated by: $\%ABS = 109 - [0.345 \times \text{topological polar surface area (TPSA)}]$ according to the method of Zhao et al. [39].

Swissadme server was also used to obtain comparative information derived from poorly and highly absorbed drugs to model human passive intestinal absorption. It works by calculating the lipophilicity and polarity of the molecules. The graphical prediction of intestinal absorption and blood–brain barrier permeation of the synthesized compounds is shown in Fig. 8. Boiled egg plot denotes bioavailable region of property space with respect to wlog P and TPSA [yellow: well penetrated within the brain with good intestinal absorption; white: intestinal absorption; gray: poor intestinal absorption]. This provides a simple visual cue for profiling new compounds in terms of their potential to be orally absorbed [40]. Inside yellow circle depicts BBB—blood brain barrier; two of the compounds are in this region. The white region which is outer to yellow depicts the human intestinal absorption. Almost all compounds lie in this white area. None of the compounds

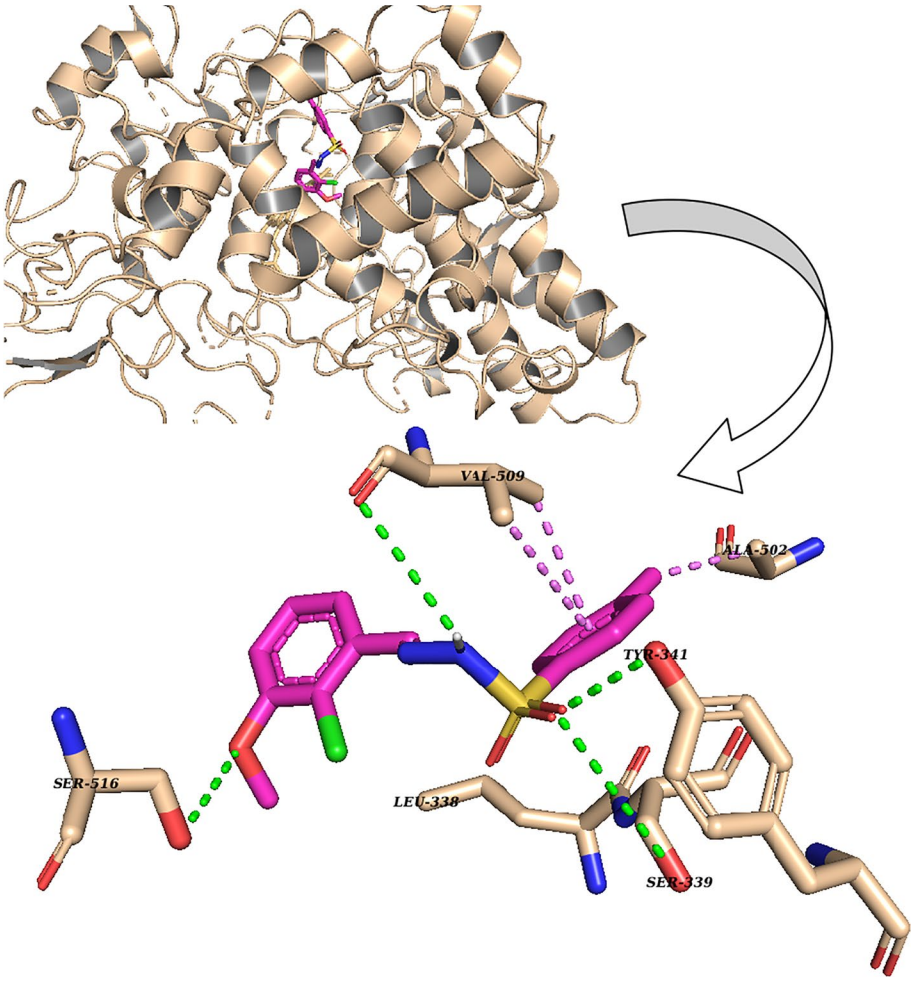

Fig. 7 Interaction of compound **3k** with COX-2 active site

are lying outside [gray area] which indicates poor intestinal absorption. The blue dots indicate that compound **3g** could be a substrate for P-glycoprotein, reducing its absorption and penetration within brain. Hence, these compounds may be said to exhibit good bioavailability. In particular, compound **3k**, the most promising agent, can be absorbed very easily by the gastrointestinal tract with no potential BBB permeability.

Conclusions

In recent years, selective and nonselective COX inhibitors have been evaluated for their effects on cancer treatment and prevention, but COX-2 selective inhibitors have become rather popular because of their lower side effects. Otherwise, the combination of COX-2 inhibitors with radiation or drug therapies may decrease their side effects in future cancer prevention and treatment.

In the current work, we described the synthesis of new sulfonylhydrazones which were investigated for their cytotoxic and apoptotic effects on PC3 and MCF-7 cell lines besides COXs activities. Compound **3k** was identified as the most potent anticancer agent in the series with IC_{50} values of 1.38 µM and 46.09 µM on PC3 and MCF-7 cell lines, respectively, and showed the highest selectivity index values. Curiously, the potent anticancer compounds showed high COX-2 inhibition percentages (up to 64%) at one dose comparable to celecoxib used as a positive control. After analysis of the results, we can deduce that a remarkable relationship exists between MTT assay results and COX-2 inhibitory activity of our compounds. The docking study showed that compound **3k** fitted well into COX-2 enzyme active site with good selectivity. Compound **3k** also induced apoptosis via the mitochondrial pathway accompanied by upregulation of Bax and downregulation of Bcl-2 protein expression. The morphological alterations of PC3 and MCF-7 cells affected by **3k** can be directly recognized by inverted microscopy. Our data demonstrate that compound **3k** may be a potential anticancer agent for further investigation in our future research. Other pathways may a possible mechanism for our molecules as anticancer agents beside COX-2 inhibition. Therefore,

Table 3 Predicted drug-likeness properties of all compounds according to OSIRIS property explorer tools

Comp.	Toxicity risks[a]				ADME properties[b]								
	M	T	IR	RE	MW ≤ 500	CLP[a] < 5	logS[a] ≥ 4	RB[b] ≤ 10	HD[b] ≤ 5	HA[b] ≤ 10	MR[b] 40-130	%Abs-	TPSA[b] ≤ 140 A
3a					354	4.39	− 3.07	4	1	7	81.68	79.55	85.37
3b					359	3.21	− 3.10	4	1	3	81.05	76.17	95.15
3c					356	4.15	− 4.36	5	1	3	98.79	76.17	95.15
3d					384	4.12	− 4.87	6	1	5	101.95	82.73	76.14
3e					377	4.07	− 3.77	5	1	6	85.49	86.16	66.91
3f					322	2.65	− 2.59	5	1	5	81.93	82.73	76.14
3g					349	1.63	− 2.74	6	1	6	90.79	66.92	121.96
3h					340	2.26	− 2.61	5	2	4	93.06	76.02	95.59
3i					383	3.28	− 3.11	5	1	4	89.67	82.73	76.14
3j					360	3.57	− 3.35	5	1	7	80.44	86.16	66.91
3k					339	3.16	− 3.01	5	1	4	86.98	82.73	76.14
3l					323	3.57	− 3.34	5	1	3	85.45	86.16	66.91
3m					354	2.50	− 2.09	4	1	4	80.97	81.47	79.80
3n					277	1.53	− 0.97	4	1	3	74.73	84.21	71.84
3o					358	3.72	− 3.28	6	1	7	82.16	82.73	76.14

: not toxic; : slightly toxic; : highly toxic

M mutagenic, *T* tumorigenic, *IR* irritant, *RE* reproductive effective, *MW* molecular weight, *CLP* cLog*P*, *S* solubility

RB: Number of rotatable bonds; HD: Number of hydrogen donors; HA: Number of hydrogen acceptors; MR: Molar refractivity; TPSA:Topological polar surface area

[a]Parameters calculated using OSIRIS Data Warrior (http://www.openmolecules.org/datawarrior/)

[b]Parameters calculated using SwissADME (http://www.swissadme.ch/).

additional mechanistic studies are also needed to understand the underlying.

Experimental

Chemistry

General

All materials used were obtained from Sigma-Aldrich (Saint Lewis, USA). Melting points were determined using the Electrothermal IA9300 apparatus and are uncorrected. FT-IR spectra were recorded on a Schimadzu FT-IR-8400S spectrometer. ^{1}H and ^{13}C-NMR spectra were recorded on Bruker 300 MHz Ultrashield TM spectrometer. Elemental analyses were determined by CHNS-932 (LECO). The liquid chromatographic system consists of an Agilent Technologies 1100 series instrument equipped with a quaternary solvent delivery system and a model Agilent series G1315 A photodiode array detector. The chromatographic data were collected and processed using Agilent Chemstation Plus software. Chromatographic separation was performed at ambient temperature using a reverse phase

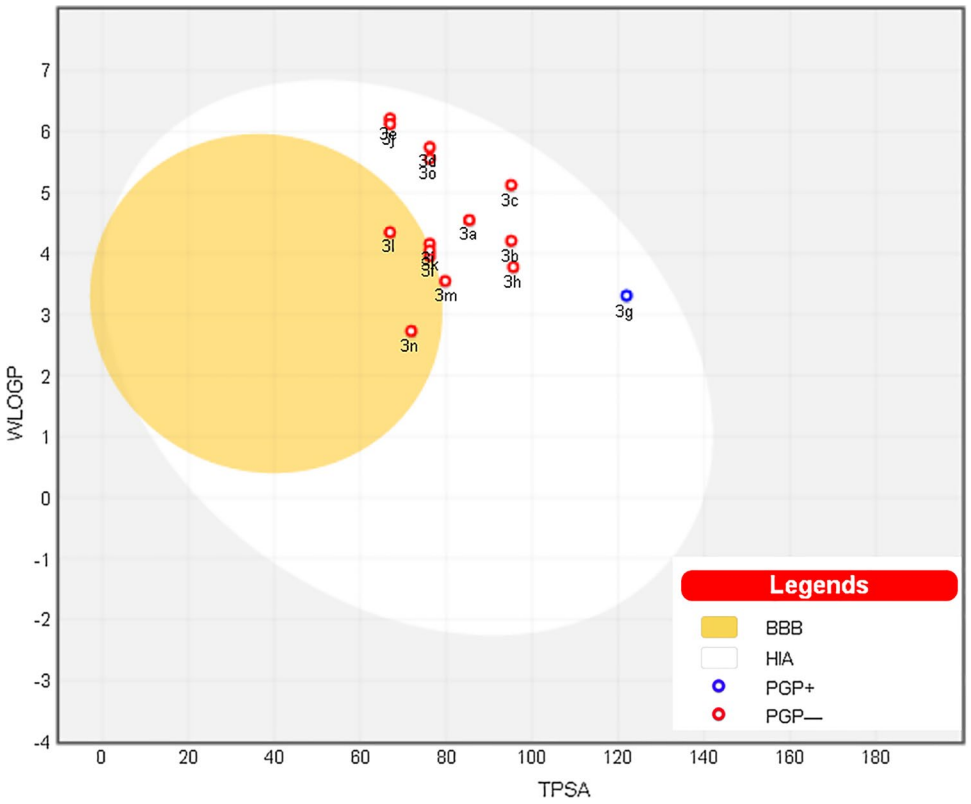

Fig. 8 Graphical distribution of compounds according to chemical classes using the boiled egg predictive model

Zorbax C8 (4.0 × 250 mm) column. All experiments were performed using acetonitrile–water (v/v, 70/30) mobile phase with UV detection at 254 nm.

General procedure for the synthesis of p-toluenesulfonyl hydrazide (2)

A mixture of p-toluenesulfonyl chloride (**1**) (26 mmol) and hydrazine hydrate (66 mmol, 99%) was stirred at 0–5 °C for 1–2 h in tetrahydrofuran (THF) (20 mL). The reaction progress and completion were monitored using TLC. After completion of the reaction, excess THF was distilled off. The product was subsequently washed with water, dried and recrystallized from ethanol [41, 42].

General procedure for the synthesis 4-methyl-*N*′-(arylmethylidene)benzensulfonohydrazide (3a-o)

A solution of *p*-toluenesulfonohydrazide **(2)** (25 mmol) was mixed with a solution of substituted aldehydes (25 mmol) in ethanol and refluxed for 3–4 h to obtain a precipitate of hydrazone which was then filtered, dried and recrystallized from ethanol [41, 42].

N′-[(2,2-difluoro-1,3-benzodioxol-5-yl) methylidene]-4-methylbenzenesulfonohydrazide (3a)

Yield 88%; m.p. 123–125 °C; HPLC t_R (min.): 5.04; FT-IR: ν/cm^{-1}: 3203 (NH), 1639 (C=N), 1369, 1161 (SO_2); ^{1}H NMR (300 MHz), (DMSO-d_6/TMS) δ ppm: 2.36 (s, 3H, Ar-C**H**$_3$); 7.41 (d, 4H, $J = 9$ Hz, Ar**H**); 7.58 (s, 1H, Ar–**H**); 7.75 (d, 2H, $J = 9$ Hz, Ar–**H**); 7.91 (s,1H, C**H**=N–); 11.54 (s,1H, SO_2N**H**–N=); ^{13}C NMR (75 MHz) (DMSO-d_6/TMS) δ ppm: 21.42 (CH_3), 107.63 (CH), 110.81 (CH), 124.73 (CH), 125.96 (C), 127.72 (2CH), 128.54 (C), 130.14 (2CH), 131.24 (C), 131.56 (C), 136.46 (N=CH), 143.97 (C-F, $J = 20$ Hz), 145.93 (C); Anal. calcd for $C_{15}H_{12}F_2N_2O_4S.1/3H_2O$ (360.331): C, 50.00; H, 3.54; N, 7.77; S, 8.90 Found: C, 49.87; H, 3.37; N, 7.56; S, 9.14.

N′-[(4-bromothiophen-2-yl) methylidene]-4-methylbenzenesulfonohydrazide (3b)

Yield 82%; m.p. 163 °C; HPLC t_R (min.): 4.71; FT-IR: ν/cm^{-1}: 3203 (NH), 1597 (C=N), 1321, 1157 (SO_2); ^{1}H NMR (300 MHz), (DMSO-d_6/TMS) δ ppm: 2.37 (s, 3H, Ar-C**H**$_3$); 7.39–7.73 (m, 6H, Ar–**H**); 8.03 (s, 1H, C**H**=N–); 11.56 (s, 1H, SO_2N**H**–N=); ^{13}C NMR (75 MHz) (DMSO-d_6/TMS) δ ppm: 21.46 (CH_3), 109.61 (C), 125.97 (CH), 126.41 (2CH), 127.64 (2CH), 132.59 (C), 136.32 (CH),

140.18 (C), 141.08 (N=CH), 144.11 (C); Anal. calcd for $C_{12}H_{11}BrN_2O_2S_2$ (359.262): C, 40.12; H, 3.09; N, 7.80; S, 17.85 Found: C, 40.45; H, 3.08; N, 7.59; S, 17.76.

4-methyl-*N*′-[(4-phenylthiophen-2-yl)methylidene] benzenesulfonohydrazide (3c)

Yield 84%; m.p. 185–186 °C; HPLC t_R (min.): 4.68; FT-IR: ν/cm^{-1}: 3186 (NH), 1610 (C=N), 1340, 1165 (SO_2); ^1H NMR (300 MHz), (DMSO-d_6/TMS) δ ppm: 2.36 (s, 3H, Ar-**C**$\mathbf{H_3}$); 7.27–7.92 (m, 11H, Ar–**H**); 8.12 (s, 1H, C**H**=N–); 11.46 (s, 1H, SO_2N**H**–N=); ^{13}C NMR (75 MHz) (DMSO-d_6/TMS) δ ppm: 21.46 (CH_3), 123.85 (CH), 126.32 (2CH), 127.67 (2CH), 127.93 (CH), 129.40 (2CH), 129.80 (CH), 130.14 (2CH), 134.83 (C), 136.44 (C), 139.51 (C), 142.08 (N=CH), 142.43 (C), 144.03 (C); Anal. calcd for $C_{18}H_{16}N_2O_2S_2$ (356.462): C, 60.65; H, 4.52; N, 7.86; S, 17.99 Found: C, 60.57; H, 4.51; N, 7.71; S, 17.96.

N′-[(4-fluoro-3-phenoxyphenyl) methylidene]-4-methylbenzenesulfonohydrazide (3d)

Yield 84%; m.p. 159–161 °C; HPLC t_R (min.): 5.74; FT-IR: ν/cm^{-1}: 3240 (NH), 1610 (C=N), 1357, 1153 (SO_2); ^1H NMR (300 MHz), (DMSO-d_6/TMS) δ ppm: 2.36 (s, 3H, Ar-**C**$\mathbf{H_3}$); 7.03 (d, 2H, $J=9$ Hz, Ar–**H**); 7.18–7.45 (m, 8H, Ar–**H**); 7.66 (d, 2H, $J=9$ Hz, Ar–**H**); 7.84 (s,1H, C**H**=N–); 11.48 (s, 1H, SO_2N**H**–N=); ^{13}C NMR (75 MHz) (DMSO-d_6/TMS) δ ppm: 21.45 (CH_3), 118.04 (2CH), 118.23 (CH), 118.42 (CH), 119.12 (CH), 124.34 (C), 127.65 (2CH), 130.09 (2CH), 130.62 (2CH), 131.72 (CH), 136.36 (C), 141.00 (C), 144.17 (N=CH), 145.70 (C), 153.03&156.35 (CF, $J=249$ Hz), 156.69 (C); Anal. calcd for $C_{20}H_{17}FN_2O_3S$ (384.424): C, 62.49; H, 4.46; N, 7.29; S, 8.34 Found: C, 62.08; H, 4.49; N, 6.67; S, 8.11.

N′-{[2-chloro-3-(trifluoromethyl)phenyl] methylidene}-4-methylbenzenesulfonohydrazide (3e)

Yield 87%; m.p. 153–155 °C; HPLC t_R (min.): 5.76; FT-IR: ν/cm^{-1}: 3147 (NH), 1595 (C=N), 1361, 1157 (SO_2); ^1H NMR (300 MHz), (DMSO-d_6/TMS) δ ppm: 2.33 (s, 3H, Ar-**C**$\mathbf{H_3}$); 7.40 (d, 2H, $J=8.1$ Hz, Ar–**H**); 7.54 (t, 1H, Ar–**H**), 7.77 (d, 2H, $J=8.1$ Hz, Ar–**H**); 7.83 (dd, 1H, $J_1=7.8$ Hz, $J_2=0.9$ Hz, Ar–**H**), 7.99 (dd, 1H, $J_1=7.8$ Hz, $J_2=0.9$ Hz, Ar–**H**), 8.33 (s, 1H, C**H**=N–); 11.96 (s, 1H, SO_2N**H**–N=); ^{13}C NMR (75 MHz) (DMSO-d_6/TMS) δ ppm: 21.42 (CH_3), 124.92 (CF_3, J=278 Hz), 125.95 (CH), 127.64 (2CH), 127.94 (CH), 129.43 (C), 130.27 (2CH), 130.63 (CH), 131.05 (C), 133.80 (C), 136.30 (C), 141.98 (N=CH), 144.26 (C); Anal. calcd for $C_{15}H_{12}ClF_3N_2O_2S.1/2C_2H_5OH$ (399.811): C, 48.06; H, 3.78; N, 7.01; S, 8.02 Found: C, 48.34; H, 3.38; N, 7.34; S, 8.92.

N′-[(4-fluoro-3-methoxyphenyl) methylidene]-4-methylbenzenesulfonohydrazide (3f)

Yield 77%; m.p. 123–125 °C; HPLC t_R (min.): 4.25; FT-IR: ν/cm^{-1}: 3155 (NH), 1595 (C=N), 1361, 1155 (SO_2); ^1H NMR (300 MHz), (DMSO-d_6/TMS) δ ppm: 2.36 (s, 3H, Ar-**C**$\mathbf{H_3}$); 3.85 (s, 3H, Ar-OC$\mathbf{H_3}$); 7.11–7.33 (m, 3H, Ar–**H**); 7.41 (d, 2H, $J=9$ Hz, Ar–**H**); 7.77 (d, 2H, $J=9$ Hz, Ar–**H**); 7.87 (s,1H, C**H**=N–); 11.46 (s,1H, SO_2N**H**–N=); ^{13}C NMR (75 MHz) (DMSO-d_6/TMS) δ ppm: 21.43 (CH_3), 58.38 (OCH_3), 111.80 (CH), 116.56 (CH), 120.31 (CH), 127.73 (2CH), 130.11 (2CH), 131.10 (C), 136.50 (C), 143.97 (C), 146.51 (N=CH), 147.77 (C), 151.35&154.64 (CF, $J=247$ Hz); Anal. calcd for $C_{15}H_{15}FN_2O_3S$ (322.354): C, 55.89; H, 4.69; N, 8.69; S, 9.95 Found: C, 55.64; H, 5.25; N, 8.11; S, 9.28.

N′-[(4-methoxy-3-nitrophenyl) methylidene]-4-methylbenzenesulfonohydrazide (3g) (CAS No: 461716-16-5)

Yield 87%; m.p. 172–173 °C; HPLC t_R (min.): 3.97; FT-IR: ν/cm^{-1}: 3147 (NH), 1620 (C=N), 1359, 1157 (SO_2); ^1H NMR (300 MHz), (DMSO-d_6/TMS) δ ppm: 2.36 (s, 3H, Ar-**C**$\mathbf{H_3}$); 3.94 (s, 3H, Ar-OC$\mathbf{H_3}$); 7.39 (d, 1H, $J=8.7$ Hz, Ar–**H**); 7.41 (d, 2H, $J=8.1$ Hz, Ar–**H**); 7.76 (d, 2H, $J=8.1$ Hz, Ar–**H**); 7.85 (dd, 1H, $J_1=8.7$ Hz, $J_2=2.1$ Hz, Ar–**H**); 7.92 (s, 1H, C**H**=N–); 8.04 (d, 1H, $J=2.1$ Hz, Ar–**H**); 11.56 (s, 1H, SO_2N**H**–N=); ^{13}C NMR (75 MHz) (DMSO-d_6/TMS) δ ppm: 21.43 (CH_3); 57.38 (OCH_3); 115.25 (CH); 123.56 (CH); 126.78 (C); 127.67 (2CH); 130.16 (2CH); 132.61 (CH); 136.48 (C); 139.72 (CH); 144.03 (C); 145.19 (–N=CH); 153.45 (C); Anal. calcd for $C_{15}H_{15}N_3O_5S$ (349.362): C, 51.57; H, 4.33; N, 12.03; S, 9.18 Found: C, 51.17; H, 4.31; N, 11.62; S, 9.55.

4-methyl-*N*′-[(3-phenyl-1*H*-pyrazol-4-yl)methylidene] benzenesulfonohydrazide (3h)

Yield 85%; m.p. 90 °C; HPLC t_R (min.): 3.67; FT-IR: ν/cm^{-1}: 3188 (NH), 1620 (C=N), 1321, 1157 (SO_2); ^1H NMR (300 MHz), (DMSO-d_6/TMS) δ ppm: 1.09 (t, CH_3 ethanol); 2.36 (s, 3H, Ar-**C**$\mathbf{H_3}$); 2.51 (m, CH_2 ethanol); 3.65 (bs, OH ethanol); 7.37–7.52 (m, 8H, Ar–**H**, C**H**=N, pyrazole N**H**), 7.72 (d, 2H, $J=9$ Hz, Ar–**H**); 7.93 (d, 2H, $J=9$ Hz, Ar–**H**); 11.01 (s,1H, SO_2N**H**–N=); ^{13}C NMR (75 MHz) (DMSO-d_6/TMS) δ ppm: 21.24 (ethanol CH_3), 21.45 (CH_3), 65.39 (ethanol CH_2), 113.71 (C), 125.97 (CH), 127.73 (2CH), 128.61 (2CH), 129.19 (C), 129.64 (2CH), 130.03 (2CH), 130.86 (CH), 136.65 (C), 141.96 (C), 143.74 (N=CH), 145.90 (C); Anal. calcd for $C_{17}H_{16}N_4O_2S.\ C_2H_5OH$ (386.467): C, 59.05; H, 5.74; N, 14.50; S, 8.30 Found: C, 58.97; H, 5.44; N, 14.53; S, 8.81.

N′-[(5-bromo-2-methoxyphenyl) methylidene]-4-methylbenzenesulfonohydrazide (3i) (CAS No: 200625-38-3)

Yield 78%; m.p. 164–166 °C; HPLC t_R (min.): 5.27; FT-IR: ν/cm^{-1}: 3159 (NH), 1595 (C=N), 1354, 1165 (SO_2); ^{1}H NMR (300 MHz), (DMSO-d_6/TMS) δ ppm: 2.36 (s, 3H, Ar-**C**$\mathbf{H_3}$); 3.79 (s, 3H, Ar-OC$\mathbf{H_3}$); 7.05 (d, 1H, $J=9$ Hz, Ar–**H**); 7.42 (d, 2H, $J=9$ Hz, Ar–**H**); 7.52 (d, 1H, $J=2.7$ Hz, Ar–**H**); 7.61 (dd, 1H, $J_1=8.7$ Hz, $J_2=2.7$ Hz, Ar–**H**); 7.73 (d, 2H, $J=9$ Hz, Ar–**H**); 8.12 (s, 1H, C**H**=N–); 11.56 (s,1H, SO_2N**H**–N=); ^{13}C NMR (75 MHz) (DMSO-d_6/TMS) δ ppm: 21.45 (CH_3), 56.51 (O-CH_3), 112.81 (C), 114.83 (CH), 124.20 (C), 127.50 (CH), 127.59 (2CH), 130.21 (2CH), 134.21 (CH), 136.52 (C), 141.22 (N=CH), 144.05 (C), 157.01 (C); Anal. calcd for $C_{15}H_{15}BrN_2O_3S$ (383.260): C, 47.01; H, 3.94; N, 7.31; S, 8.37 Found: C, 47.25; H, 4.08; N, 7.04; S, 8.45.

N′-{4-fluoro-2-(trifluoromethyl)phenyl] methylidene}-4-methylbenzenesulfonohydrazide (3j)

Yield 82%; m.p. 165–166 °C; HPLC t_R (min.): 6.14; FT-IR: ν/cm^{-1}: 3211 (NH), 1597 (C=N), 1319, 1155 (SO_2); ^{1}H NMR (300 MHz), (DMSO-d_6/TMS) δ ppm: 2.37 (s, 3H, Ar-**C**$\mathbf{H_3}$); 7.42 (d, 2H, $J=9$ Hz, Ar–**H**); 7.59 (t, 1H, Ar–**H**); 7.67 (dd, 1H, $J_1=9$ Hz, $J_2=2.7$ Hz, Ar–**H**); 7.77 (d, 2H, $J=9$ Hz, Ar–**H**); 7.97 (dd, 1H, $J_1=9$ Hz, $J_2=2.7$ Hz, Ar–**H**); 8.16 (s, 1H, C**H**=N–); 11.88 (s,1H, SO_2N**H**–N=); ^{13}C NMR (75 MHz) (DMSO-d_6/TMS) δ ppm: 21.38 (CH_3), 144.24 (CH), 120.52&121.58 (CH, J = 21 Hz), 123.4 (CF_3, J = 273 Hz), 127.55 (2CH), 128.17 (C), 129.01 (C), 129.78 (CH), 130.22 (2CH), 136.33 (C), 141.18 (C), 144.14 (N=CH), 160.90 &164.22 (C-F, J = 249 Hz); Anal. calcd for $C_{15}H_{12}F_4N_2O_2S$ (360.326): C, 50.00; H, 3.36; N, 7.77; S, 8.90 Found: C, 49.74; H, 3.67; N, 7.70; S, 9.23.

N′-[(2-chloro-3-methoxyphenyl) methylidene]-4-methylbenzenesulfonohydrazide (3k)

Yield 80%; m.p. 161–163 °C; HPLC t_R (min.): 4.68; FT-IR: ν/cm^{-1}: 3157 (NH), 1597 (C=N), 1354, 1157 (SO_2); ^{1}H NMR (300 MHz), (DMSO-d_6/TMS) δ ppm: 2.97 (s, 3H, Ar-**C**$\mathbf{H_3}$); 3.85 (s, 3H, Ar-OC$\mathbf{H_3}$); 7.149–7.345 (m, 3H, Ar–**H**); 7.42 (d, 2H, $J=9$ Hz, Ar–**H**); 7.75 (d, 2H, $J=9$ Hz, Ar–**H**); 8.27 (s,1H, C**H**=N–); 11.75 (s, 1H, SO_2N**H**–N=); ^{13}C NMR (75 MHz) (DMSO-d_6/TMS) δ ppm: 21.45 (CH_3), 58.76 (OCH_3), 114.08 (CH), 118.34 (CH), 121.73 (CH), 127.64 (2CH), 128.34 (CH), 130.23 (2CH), 132.43 (C), 138.45 (C), 143.37 (C), 144.11 (N=CH), 156.32 (C); Anal. calcd for $C_{15}H_{15}ClN_2O_3S$ (338.809): C, 53.17; H, 4.46; N, 8.27; S, 9.46 Found: C, 53.28; H, 4.48; N, 8.09; S, 9.80.

N′-[(2-chloro-6-methylphenyl) methylidene]-4-methylbenzenesulfonohydrazide (3l)

Yield 76%; m.p. 175–176 °C; HPLC t_R (min.): 5.42; FT-IR: ν/cm^{-1}: 3201 (NH), 1589 (C=N), 1373, 1161 (SO_2); ^{1}H NMR (300 MHz), (DMSO-d_6/TMS) δ ppm: 2.18 (s, 3H, Ar-**C**$\mathbf{H_3}$); 2.37 (s, 3H, Ar-**C**$\mathbf{H_3}$); 7.17–7.33 (m, 3H, Ar–**H**); 7.41 (d, 2H, $J=9$ Hz, Ar–**H**); 7.75 (d, 2H, $J=9$ Hz, Ar–**H**); 8.25 (s, 1H, C**H**=N–); 11.70 (s, 1H, SO_2NH–N=); ^{13}C NMR (75 MHz) (DMSO-d_6/TMS) δ ppm: 21.46 (CH_3), 21.86 (CH_3), 127.76 (CH), 127.80 (2CH), 128.53 (CH), 129.93 (CH), 130.14 (2CH), 130.64 (C), 131.23 (C), 136.47 (C), 139.63 (C), 144.07 (C), 145.13 (N=CH); Anal. calcd for $C_{15}H_{15}ClN_2O_2S$ (322.809): C, 55.81; H, 4.68; N, 8.68; S, 9.93 Found: C, 55.25; H, 4.79; N, 8.35; S, 9.28.

N′-[(6-bromopyridin-2-yl) methylidene]-4-methylbenzenesulfonohydrazide (3m)

Yield 88%; m.p. 117–119 °C; HPLC t_R (min.): 4.17; FT-IR: ν/cm^{-1}: 3203 (NH), 1597 (C=N), 1361, 1159 (SO_2); ^{1}H NMR (300 MHz), (DMSO-d_6/TMS) δ ppm: 2.36 (s, 3H, Ar-**C**$\mathbf{H_3}$); 7.10–7.80 (m, 7H, Ar–**H**); 7.82 (s, 1H, C**H**=N–); 11.98 (s, 1H, SO_2N**H**–N=); ^{13}C NMR (75 MHz) (DMSO-d_6/TMS) δ ppm: 21.47 (CH_3), 119.46 (CH), 127.63 (2CH), 129.05 (CH), 130.29 (2CH), 136.34 (CH), 140.69 (C), 141.40 (C), 144.24 (N=CH), 145.145 (C), 154.04 (C); Anal. calcd for $C_{13}H_{12}BrN_3O_2S$ (354.222): C, 44.08; H, 3.41; N, 10.86; S, 9.05 Found: C, 44.40; H, 3.57; N, 10.73; S, 8.34.

N′-[(1-methyl-1*H*-pyrrol-2-yl) methylidene]-4-methylbenzenesulfonohydrazide (3n) (CAS No: 113334-34-2)

Yield 68%; m.p. 124 °C; HPLC t_R (min.): 3.95; FT-IR: ν/cm^{-1}: 3157 (NH), 1618 (C=N), 1350, 1165 (SO_2); ^{1}H NMR (300 MHz), (DMSO-d_6/TMS) δ ppm: 2.36 (s, 3H, Ar-**C**$\mathbf{H_3}$); 3.64 (s, 3H, N-**C**$\mathbf{H_3}$); 6.00–6.87 (m, 3H, Ar**–H**); 7.40 (d, 2H, $J=8.1$ Hz, Ar–**H**); 7.72(d, 2H, $J=8.4$ Hz, Ar–**H**); 7.78 (s, 1H, C**H**=N–); 10.92 (s, 1H, SO_2N**H**–N=); ^{13}C NMR (75 MHz) (DMSO-d_6/TMS) δ ppm: 21.40 (CH_3), 36.58 (CH_3), 108.48 (CH), 115.60 (CH), 126.71 (CH), 127.76 (2CH), 128.56 (C), 129.35 (2CH), 136.40 (C), 141.37 (N=CH), 143.74 (C); Anal. calcd for $C_{13}H_{15}N_3O_2S$ (277.342): C, 56.30; H, 5.45; N, 15.15; S, 11.56 Found: C, 56.40; H, 5.18; N, 14.68; S, 11.36

***N′*-{[2-(trifluoromethoxy)phenyl] methylidene}-4-methylbenzenesulfonohydrazide (3o)**

Yield 74%; m.p. 139–140 °C; HPLC t_R (min.): 5.41; FT-IR: ν/cm^{-1}: 3142 (NH), 1606 (C=N), 1361, 1157 (SO_2); ^1H NMR (300 MHz), (DMSO-d_6/TMS) δ ppm: 2.36 (s, 3H, Ar-**CH_3**); 7.41–7.81 (m, 8H, Ar**–H**); 8.12 (s, 1H, C**H**=N–); 11.74 (s, 1H, SO_2N**H**–N=); ^{13}C NMR (75 MHz) (DMSO-d_6/TMS) δ ppm: 21.43 (CH_3), 118.73 (CH), 122.19 (CH), 125.96 (CH), 126.90 (C), 127.04 (CH), 127.62 (2CH), 128.51 (C), 130.21 (2CH), 132.21 (C), 136.44 (N=CH), 142.30 (CF_3), 146.85 (C); Anal. calcd for $C_{15}H_{13}N_2O_3S$ (358.335): C, 50.28; H, 3.66; N, 7.82; S, 8.95 Found: C, 50.02; H, 3.67; N, 7.52; S, 9.21

Molecular modeling studies

Preparation of ligands

The synthesized compounds **3a–o** and reference ligand (celecoxib) were drawn with the Spartan 04 software (SPARTAN 04, Wavefunction, Inc., Irvine, USA) and optimized for each compound by using the semi-empirical PM3 method. For each compound, the most stable conformation was utilized in docking calculation and The AutoDock Tools program was used to generate the docking input files [43].

Preparation of COXs structures for docking studies

The structures of COX-1 (PDB code: 3KK6, resolution: 2.75 Å) COX-2 (PDB code: 3LN1, resolution: 2.4 Å) were obtained from the protein databank [44, 45]. Water molecules and co-crystallized inhibitor celecoxib were deleted together with *N*-acetyl-D-glucosamine and β-octylglucoside in the structure; at the same time, the charge of the Fe atom was set to + 2 manually. This structure was protonated using the AutoDock Tools program, and thereafter the obtained structure was energy-minimized.

Docking studies

AutoDock Vina software was used for the synthesized compounds **3a–o** into the COX-1 and COX-2 structures docking calculations [46]. The size of binding pocket was detected 40 × 40 × 40 points for both enzymes. For COX-2 enzyme, *x* (30.518), *y* (− 21.298) and *z* (− 16.69) dimensions were built, while *x* (− 31.867), *y* (42.146) and *z* (− 5.089) dimensions were used in COX-1 enzyme docking studies, appropriate to the position of celecoxib in these structures. The Vina parameter "exhaustiveness" was set to the value of 10; besides a grid spacing of 0.375 Å was employed for the calculation of the energetic map for both docking studies. The molecular docking protocol was validated by re-docking of the co-crystallized inhibitor celecoxib back into respective enzymes COX-1 and COX-2 with 0.8 Å and 0.7 Å root mean square deviation (RMSD) values. During study of validations as well as our docking of ligands was used flexible ligand in rigid protein. The results files were analyzed using Accelrys Discovery Studio Visualizer 4.0 program and PyMOL Molecular Graphics System.

Biological assays

Cell culture and cell viability assay

Cell lines were purchased from the American Type Culture Collection (ATCC, Manassas, VA, USA). Human breast cancer cell line MCF-7, human prostate cancer cell line PC3, and mouse fibroblast cell line L929 cells were maintained in Dulbecco's modified Eagle's medium (DMEM, Invitrogen) or RPMI-1640 supplemented with 10% FBS, 2 mM l-glutamine, 100 U/mL penicillin, and 100 µg/mL streptomycin and kept in a humidified atmosphere at 37 °C incubator with 5% CO_2 in air. To determine the cell viability, cells were plated onto 96-well plates (1×10^4 cells/well). The cells were treated with different concentrations (0, 0.1, 1, 10, 100 and 1000 µM) of synthesized compound **(3a–o)** incubated for 24 h. After the incubation, cells were washed with PBS and added to 100 µL DMEM/RPMI-1640. A total of 10 µL of the MTT (3-(4,5-dimethylthiazol-2-yl)-2,5-diphenyltetrazolium bromide) (Vybrant, Invitrogen) labeling reagent was added to each well and incubated for 4 h in humidified atmosphere at 37 °C incubator with 5% CO_2 in air. After the incubation, 100 µL of the SDS buffer was added into each well for solubilization of formazan precipitate. Then, absorbance was measured by microplate reader at 570 nm and was carried out in triplicate of each assay [47].

Cell growth assays

In order to investigate the effects of compound **3k** on cell survival of PC3 and MCF-7 cancer cell lines, cells were seeded in 24-well plates and incubated with compounds at a final concentration of IC_{50} in growth medium (without antibiotics) for 12 h, 24 h and 48 h. After the incubation, methylene blue staining was used for cell survivals. The cells were extracted with 1% SDS in PBS solution and stained with 0.01% methylene blue solutions. The absorbance was measured at 600 nm with microplate reader. Each experiment was repeated three times.

Western blot analysis for protein expression

Cells were treated with final concentration of IC_{50} of synthesized compound **3k** in 6 well plates and incubated for 24 h. Cells were lysed using RIPA cell lysis buffer (89900, Thermo), and the protein concentrations were determined by the BCA protein assay (Thermo Scientific). Samples were denaturated with Laemli buffer, and 25 µg protein was loaded to each well. The samples were resolved by 4–12% sodium dodecyl sulfate–polyacrylamide gel electrophoresis and were transferred to polyvinylidene fluoride membrane, which was then blocked with 3% BSA (Capricorn Scientific, BSA-1T) in Tris buffered saline (TBS). The membrane was washed twice in TBS containing Tween-20 (0.1%) and incubated overnight with primary antibodies (1:500 dilution anti-Bax sc-7480, anti-Bcl2 sc-492, anti-GAPDH sc-25778, Santa Cruz Biotechnology, Heidelberg, Germany) and washed with TBS containing Tween-20 (0.1%). The membrane was washed and then incubated with horseradish peroxidase conjugated secondary antibody (anti-mouse; sc-2060 or anti-rabbit; sc-2004, Santa Cruz Biotechnology) for 2 h. The blots were developed with chemiluminescence reagents (sc2048, Santa Cruz Biotechnology, Texas, USA) and analyzed with chemiluminescent imaging systems (Syngene, Cambridge, UK). Data were analyzed using "Image J Programme Optical Density Analysis Software" (NIH) by measuring each band three times for quantification. Signals were normalized with respect to GAPDH.

In vitro COX inhibition assay

In order to determine the COX activity, inhibitors were dissolved in DMSO. Using a commercial COX (ovine/human) inhibitor screening assay kit (Cayman 560131, USA) and following the manufacturer's instructions, compounds was used for measuring COX inhibition assay. Celecoxib was used as the reference drug for comparison of activity.

Acknowledgements This work was supported by the Research Fund of Marmara University, Project Number: SAG-K-120917-0495.

Compliance with ethical standards

Conflict of interest The authors have declared no conflict of interest.

References

1. Carmichael J (1994) Cancer chemotherapy: identifying novel anticancer drugs. Br Med J 308:1288–1290. https://doi.org/10.1136/bmj.308.6939.1288
2. Hunter AM, Lacasse ÆEC, Korneluk ÆRG (2007) The inhibitors of apoptosis (IAPs) as cancer targets. Apoptosis 12:1543–1568. https://doi.org/10.1007/s10495-007-0087-3
3. Ashe PC, Berry MD (2003) Apoptotic signaling cascades. Prog Neuropsychopharmacol Biol Psychiatry 308:199–214. https://doi.org/10.1016/S0278-5846(03)00016-2
4. Kumar R, Herbert PE, Warrens AN (2005) An introduction to death receptors in apoptosis. Int J Surg 3:268–277. https://doi.org/10.1016/j.ijsu.2005.05.002
5. Elumalai P, Gunadharini DN, Senthilkumar K et al (2012) Induction of apoptosis in human breast cancer cells by nimbolide through extrinsic and intrinsic pathway. Toxicol Lett 215:131–142. https://doi.org/10.1016/j.toxlet.2012.10.008
6. Sfanos KS, De Marzo AM (2014) Prostate cancer and inflammation: the evidence. Histopathology 60:199–215. https://doi.org/10.1111/j.1365-2559.2011.04033.x
7. Morrow RJ, Etemadi N, Yeo B, Ernst M (2017) Challenging a misnomer? The role of inflammatory pathways in inflammatory breast cancer. Mediators Inflamm 2017:4754827. https://doi.org/10.1155/2017/4754827
8. Liu B, Qu L, Yan S (2015) Cyclooxygenase-2 promotes tumor growth and suppresses tumor immunity. Cancer Cell Int 15:106. https://doi.org/10.1186/s12935-015-0260-7
9. Harris RE, Casto BC, Harris ZM (2014) Cyclooxygenase-2 and the inflammogenesis of breast cancer. World J Clin Oncol 5:677–692. https://doi.org/10.5306/wjco.v5.i4.677
10. Gupta S, Srivastava M, Ahmad N et al (2000) Over-expression of cyclooxygenase-2 in human prostate adenocarcinoma. Prostate 42:73–78. https://doi.org/10.1002/(SICI)1097-0045(20000101)42:1%3c73:AID-PROS9%3e3.0.CO;2-G
11. Maekawa M, Sugan K, San H et al (1998) Increased expression of cyclooxygenase-2 to -1 in human colorectal cancers and adenomas, but not in hyperplastic polyps. Jpn J Clin Oncol 28:421–426. https://doi.org/10.1093/jjco/28.7.421
12. Meric J-B, Rottey S, Olaussen K et al (2006) Cyclooxygenase-2 as a target for anticancer drug development. Crit Rev Oncol Hematol 59:51–64. https://doi.org/10.1016/j.critrevonc.2006.01.003
13. Rollas S, Küçükgüzel SG (2007) Biological activities of hydrazone derivatives. Molecules 12:1910–1939. https://doi.org/10.3390/12081910
14. Aydın S, Kaushik-basu N, Arora P et al (2013) Microwave assisted synthesis of some novel Flurbiprofen hydrazide- hydrazones as anti-HCV NS5B and anticancer agents. Marmara Pharm J 17:26–34. https://doi.org/10.12991/201317389
15. Çıkla P, Özsavcı D, Bingöl-Özakpınar Ö et al (2013) Synthesis, cytotoxicity, and pro-apoptosis activity of etodolac hydrazide derivatives as anticancer agents. Arch Pharm (Weinheim) 346:367–379. https://doi.org/10.1002/ardp.201200449
16. Küçükgüzel ŞG, Koç D, Çıkla-Süzgün P et al (2015) Synthesis of tolmetin hydrazide-hydrazones and discovery of a potent apoptosis inducer in colon cancer cells. Arch Pharm (Weinheim) 348:730–742. https://doi.org/10.1002/ardp.201500178
17. Şenkardeş S, Kaushik-basu N, Durmaz İ et al (2016) Synthesis of novel diflunisal hydrazide hydrazones as anti-hepatitis C virus agents and hepatocellular carcinoma inhibitors. Eur J Med Chem 108:301–308. https://doi.org/10.1016/j.ejmech.2015.10.041
18. Tatar E, Şenkardeş S, Sellitepe E et al (2016) Synthesis, and prediction of molecular properties and antimicrobial activity of some acylhydrazones derived from *N*-(arylsulfonyl) methionine. Turk J Chem 40:510–534. https://doi.org/10.3906/kim-1509-21
19. Siemann S, Evanoff DP, Marrone L et al (2002) N-Arylsulfonyl hydrazones as inhibitors of IMP-1 metallo-β-lactamase. Antimicrob Agents Chemother 46:2450–2457. https://doi.org/10.1128/aac.46.8.2450-2457.2002
20. Gao Z, Lv M, Li Q, Xu H (2015) Synthesis of heterocycle-attached methylidenebenzenesulfonohydrazones as antifungal agents.

Bioorg Med Chem Lett 25:5092–5096. https://doi.org/10.1016/j.bmcl.2015.10.017
21. Begum F, Almandil NB, Lodhi MA et al (2019) Synthesis and urease inhibitory potential of benzophenone sulfonamide hybrid in vitro and in silico. Bioorg Med Chem 27:1009–1022. https://doi.org/10.1016/j.bmc.2019.01.043
22. Mobasher S, Abid A, Amna H et al (2017) Sulfonyl hydrazones derived from 3-formylchromone as non-selective inhibitors of MAO-A and MAO-B:Synthesis, molecular modelling and in silico ADME evaluation. Bioorg Chem 75:291–302. https://doi.org/10.1016/j.bioorg.2017.10.001
23. Hayakawa M, Kawaguchi K, Kaizawa H et al (2007) Synthesis and biological evaluation of sulfonylhydrazone- substituted imidazo [1,2-a] pyridines as novel PI3 kinase p110 a inhibitors. Bioorg Med Chem 15:5837–5844. https://doi.org/10.1016/j.bmc.2007.05.070
24. Wei D, Pan Y, Wang H et al (2018) Synthesis of substituted aromatic heterocyclic sulfonyl hydrazone compounds and in vitro anti-hepatoma activity: preliminary results. Eur Rev Med Pharmacol Sci 22:4720–4729. https://doi.org/10.26355/eurrev_201807_15532
25. George RF (2018) Facile synthesis of simple 2-oxindole-based compounds with promising antiproliferative activity. Future Med Chem 10:269–282. https://doi.org/10.4155/fmc-2017-0148
26. Korcz M, Franciszek S, Bednarski PJ, Kornicka A (2018) Cytotoxic properties of novel quinoline-3-carbaldehyde hydrazones bearing a 1,2,4-triazole or benzotriazole moiety. Molecules 23:1497. https://doi.org/10.3390/molecules23061497
27. Yu Y, Huang W, Chen Y et al (2016) Calcium carbide as the acetylide source: transition-metal-free synthesis of substituted pyrazoles via [1,5]-sigmatropic rearrangements. Green Chem 18:6445–6449. https://doi.org/10.1039/c6gc02776h
28. Katsuhiro S, Hiraku I (1987) Thermolysis of sodium salts of tosylhydrazones of some heterocyclic aldehydes in the presence of silver chromate: 1,3 N→C migration of tosyl group. Heterocycles 26:2–9. https://doi.org/10.3987/R-1987-07-1891
29. Kısmet K, Akay MT, Abbasoğlu O, Ercan A (2004) Celecoxib: a potent cyclooxygenase-2 inhibitor in cancer prevention. Cancer Detect Prev 28:127–142. https://doi.org/10.1016/j.cdp.2003.12.005
30. Hsu A, Ching T, Wang D et al (2000) The Cyclooxygenase-2 inhibitor celecoxib induces apoptosis by blocking Akt activation in human prostate cancer cells independently of Bcl-2*. J Biol Chem 275:11397–11403. https://doi.org/10.1074/jbc.275.15.11397
31. Altaf M, Casagrande N, Mariotto E et al (2019) Potent in vitro and in vivo anticancer activity of new bipyridine and bipyrimidine gold (III) dithiocarbamate derivatives. Cancers 11:1–14. https://doi.org/10.3390/cancers11040474
32. Dai Z, Ma X, Kang H et al (2012) Antitumor activity of the selective cyclooxygenase-2 inhibitor, celecoxib, on breast cancer in vitro and in vivo. Cancer Cell Int 12:1–8. https://doi.org/10.1186/1475-2867-12-53
33. Patel MI, Subbaramaiah K, Du B et al (2007) Celecoxib inhibits prostate cancer growth: evidence of a cyclooxygenase-2-independent mechanism. Clin Cancer Res 11:1999–2007. https://doi.org/10.1158/1078-0432.CCR-04-1877
34. Grösch S, Tegeder I, Niederberger E et al (2001) COX-2 independent induction of cell cycle arrest and apoptosis in colon cancer cells by the selective COX-2 inhibitor celecoxib. FASEB J 15:2742–2744. https://doi.org/10.1096/fj.01-0299fje
35. Wang Z, Chen J, Liu J (2014) COX-2 Inhibitors and gastric cancer. Gastroent Res Pract 2014:132320. https://doi.org/10.1155/2014/132320
36. Morrow D, Daniel R, Dubois N (1998) Modulation of apoptosis and Bcl-2 expression by prostaglandin E2 in human colon cancer cells. Cancer Res 58:362–366
37. Abdelazeem AH, Gouda AM, Omar HA, Tolba MF (2014) Design, synthesis and biological evaluation of novel diphenylthiazole-based cyclooxygenase inhibitors as potential anticancer agents. Bioorg Chem 57:132–141. https://doi.org/10.1016/j.bioorg.2014.10.001
38. Murakami M (2011) Lipid mediators in life science. Exp Anim 60:7–20. https://doi.org/10.1538/expanim.60.7
39. Zhao YH, Abraham MH, Le J et al (2015) Rate-limited steps of human oral absorption and QSAR studies. Pharm Res 19:1446–1457. https://doi.org/10.1023/A:1020444330011
40. Daina A, Zoete V (2016) A BOILED-Egg to predict gastrointestinal absorption and brain penetration of small molecules. ChemMedChem 11:1117–1121. https://doi.org/10.1002/cmdc.201600182
41. Neumann DM, Cammarata A, Backes G et al (2015) Synthesisand anti fungal activity of substituted 2,4,6-pyrimidinetrione carbalde hydehydrazones. Bioorg Med Chem 22:813–826. https://doi.org/10.1016/j.bmc.2013.12.010
42. Murtaza S, Shamim S, Kousar N et al (2015) Synthesis, biological investigation, calf thymus DNAbinding and docking studies of the sulfonyl hydrazides and their derivatives. J Mol Struct 1107:99–108. https://doi.org/10.1016/j.molstruc.2015.11.046
43. Morris GM, Huey R, Lindstrom W et al (2009) AutoDock4 and AutoDockTools4: automated docking with selective receptor flexibility. J Comput Chem 30:2785–2791. https://doi.org/10.1002/jcc.21256
44. Rimon G, Sidhu RS, Lauver DA et al (2010) Coxibs interfere with the action of aspirin by binding tightly to one monomer of cyclooxygenase-1. PNAS 107:28–33. https://doi.org/10.1073/pnas.0909765106
45. Wang JL, Limburg D, Graneto MJ et al (2010) The novel benzopyran class of selective cyclooxygenase-2 inhibitors. Part 2: the second clinical candidate having a shorter and favorable human half-life. Bioorg Med ChemLett 20:7159–7163. https://doi.org/10.1016/j.bmcl.2010.07.054
46. Trott O, Olson AJ (2009) AutoDock Vina: improving the speed and accuracy of docking with a new scoring function, efficient optimization, and multithreading. J Comput Chem 31:455–461. https://doi.org/10.1002/jcc.21334
47. Çoruh I, Çevik Ö, Yelekçi K et al (2018) Synthesis, anticancer activity, and molecular modeling of etodolac-thioether derivatives as potentmethionine aminopeptidase (type II) inhibitors. Arch Pharm (Weinheim) 351:e1700195. https://doi.org/10.1002/ardp.201700195